

## Research Article

# Photocatalytic Reduction of CO<sub>2</sub> to Methane on Pt/TiO<sub>2</sub> Nanosheet Porous Film

Li Qiu-ye, Zong Lan-lan, Li Chen, Cao Yu-hui, Wang Xiao-dong, and Yang Jian-jun

Key Laboratory for Special Functional Materials, Henan University, Kaifeng 475004, China

Correspondence should be addressed to Li Qiu-ye; qiuyeli@henu.edu.cn

Received 13 March 2014; Accepted 24 March 2014; Published 13 April 2014

Academic Editor: Haimin Zhang

Copyright © 2014 Li Qiu-ye et al. This is an open access article distributed under the Creative Commons Attribution License, which permits unrestricted use, distribution, and reproduction in any medium, provided the original work is properly cited.

Anatase TiO<sub>2</sub> nanosheet porous films were prepared by calcination of the orthorhombic titanate acid films at 400°C. They showed an excellent photocatalytic activity for CO<sub>2</sub> photoreduction to methane, which should be related to their special porous structure and large Brunauer-Emmett-Teller (BET) surface area. In order to further improve the photocatalytic activity, Pt nanoparticles were loaded uniformly with the average size of 3-4 nm on TiO<sub>2</sub> porous films by the photoreduction method. It was found that the loading of Pt expanded the light absorption ability of the porous film and improved the transformation efficiency of CO<sub>2</sub> to methane. The conversion yield of CO<sub>2</sub> to methane on Pt/TiO<sub>2</sub> film reached 20.51 ppm/h·cm<sup>2</sup>. The Pt/TiO<sub>2</sub> nanosheet porous film was characterized by means of X-ray diffraction (XRD), scanning electron microscopy (SEM), transmission electron microscope (TEM), and ultraviolet-visible light diffuse reflectance spectra (UV-vis DRS). Moreover, the transient photocurrent-time curves showed that the Pt/TiO<sub>2</sub> nanosheet porous film exhibited higher photocurrent, indicating that the higher separation efficiency of the photogenerated charge carriers was achieved.

## 1. Introduction

Fossil fuels are our primary source of energy. Unfortunately, CO<sub>2</sub> emissions generated in using these fuels have drastically increased in atmosphere in recent years, and the fast-growing CO<sub>2</sub> leads to climate change, which has become one of the greatest threats of environmental problems. It is very urgent to reduce the accumulation of CO<sub>2</sub> in the atmosphere. In general, the photocatalytic reduction of CO<sub>2</sub> is a possible avenue to convert CO<sub>2</sub> into hydrocarbon fuels, because reducing the amount of CO<sub>2</sub> will not only meet the purpose of environmental protection but also provide raw materials for chemical industry. This process utilizes ultraviolet (UV) and/or visible light as the excitation source for semiconductor catalysts, and the photoexcited electrons reduce CO<sub>2</sub> with H<sub>2</sub>O on the catalyst surface and form energy-bearing products such as carbon monoxide (CO), methane (CH<sub>4</sub>), methanol (CH<sub>3</sub>OH), formaldehyde (HCHO), and formic acid (HCOOH) [1].

Many researchers [2] have shown that CO<sub>2</sub> could be reduced by water vapor or solvent with photocatalysts. Among these photocatalysts, TiO<sub>2</sub> or TiO<sub>2</sub>-based materials

may promote the photoreduction of CO<sub>2</sub> to useful organic compounds [3–9]. Moreover, TiO<sub>2</sub> is one of the most intensively studied and widely used photocatalysts as a result of a number of advantageous features such as low cost, relatively high catalytic activity, low toxicity, and high chemical stability [10–12]. Especially modification of TiO<sub>2</sub> through noble metal supporting is increasingly being considered for maximising its photocatalytic efficiency. These metals may facilitate electron-hole separation and promote interfacial electron transfer or they may decrease the TiO<sub>2</sub> band gap, which benefits electrons transfer from the valence band to the conduction band, facilitating the formation of oxidative species. The TiO<sub>2</sub>-based nanomaterials, especially the titanate network films, obtained by the hydrothermal method often have large BET surface area and strong adsorption ability [13]. It is noticeable that the surface network structure of the film can enhance the adsorption of the reactive species and absorption efficiency of the incident light and further improve the photocatalytic activity [14–16].

Herein, anatase TiO<sub>2</sub> nanosheet porous films were obtained by calcination of the orthorhombic titanate acid films at 400°C. Because the surface of titanate acid consists of

the porous network structure [17], the obtained anatase  $\text{TiO}_2$  has stronger absorption ability and higher photocatalytic performance compared with the film prepared by sol-gel method in the same condition. Moreover, it is noticeable that the porous structure of the film also can enhance the adsorption of the reactive species and absorption efficiency of the incident light [14–16]. In order to further improve the photocatalytic activity, Pt nanoparticles were loaded on the surface of it as an electron trapper to capture the photogenerated electrons by the photoreduction method. The relationship between the morphology, structure, and their photocatalytic activity was investigated in detail.

## 2. Experimental

### 2.1. Preparation of $\text{TiO}_2$ and Pt- $\text{TiO}_2$ Nanosheet Porous Films.

The precursor for preparing  $\text{TiO}_2$  porous film was titanate nanotube (TAN) porous film, and the typical preparing process of TAN film was as follows: a Ti thin foil with a size of  $2 \times 4 \text{ cm}^2$  was put into 100 mL of 10 M NaOH aqueous solution, followed by the hydrothermal treatment in a 120 mL Teflon-lined autoclave at  $120^\circ\text{C}$  for 24 h. After cooling down, the obtained titanate network film was washed with distilled water several times and then immersed in a 0.1 M HCl aqueous solution overnight. After that, the product was washed several times with water and then dried in the  $\text{N}_2$  stream.

$\text{TiO}_2$  nanosheet porous films were prepared by calcination of TAN films at  $400^\circ\text{C}$  for 4 h in air. Then, Pt nanoparticles were loaded by the photoreduction method in  $\text{H}_2\text{PtCl}_6$  ethanol solution. The solution was illuminated under UV light for 1 h. After that, the sample was washed with deionized water and dried. For a comparison, a  $\text{TiO}_2$  film prepared by a sol-gel method was used as a reference [18]; the sample was denoted by R- $\text{TiO}_2$ .

**2.2. Characterization.** UV-vis diffuse reflectance spectra (DRS) were obtained on a Shimadzu U-3010 spectrometer, using  $\text{BaSO}_4$  as a reference. X-ray diffraction (XRD) patterns were measured on an X'Pert Philips diffractometer (Cu  $\text{K}\alpha$  radiation;  $2\theta$  range  $5\text{--}90^\circ$ , step size  $0.08^\circ$ , accelerating voltage 40 kV, and applied current 40 mA). The particle size and surface morphology of the samples were observed using a scanning electron microscope (SEM) (JSM-7100F, JEOL Co., Japan) and transmission electron microscope (TEM) (JEM-2010, JEOL Co., Japan).

**2.3. Photoelectrochemical Measurements.** The transient photocurrent-time ( $I$ - $t$ ) experiments were conducted using a conventional three-electrode system on the electrochemical analyzer (IM6ex, Germany). The photocatalyst film served as the working electrode, and a Pt meshwork and an Ag/AgCl electrode (SCE) acted as the counter electrode and reference electrode, respectively. The electrolyte was  $\text{Na}_2\text{SO}_4$  with a concentration of  $0.5 \text{ mol}\cdot\text{L}^{-1}$ .

**2.4. Photocatalytic Activity Evaluation.** The photocatalytic reduction of  $\text{CO}_2$  was conducted in a flat closed reactor

with the inner capacity of 358 mL containing 20 mL 0.1 mol/L  $\text{KHCO}_3$  solution. The prepared  $\text{TiO}_2$  nanosheet porous film was located in the center of the reactor and then the ultrapure gaseous  $\text{CO}_2$  and water vapor was flowed through the reactor for 2 h to achieve the adsorption-desorption equilibrium. Before illumination, the reactor was sealed. The light source was the high pressure Hg lamp with 300 W, and the intensity of the incident light was measured to be  $10.4 \text{ mW}/\text{cm}^2$ . The photocatalytic reaction was typically performed at room temperature for 6 h. The products were measured by gas chromatography (GC). The comparison tests consisted of a reaction under light without the catalysts and a reaction in dark with the catalysts. The results indicated that there was almost no methane production in the comparison experiments.

## 3. Results and Discussions

**3.1. Phase Structure, Morphology, and Optical Absorption of Pt-Loaded  $\text{TiO}_2$  Nanosheet Porous Film.** The phase structure of the titania films was analyzed by the XRD technique. As shown in Figure 1(a), the  $\text{TiO}_2$  film belongs to the typical anatase phase. In our previous work, we knew that TAN precursor belonged to the orthorhombic system [19]. This indicated that the orthorhombic TAN has been transformed to anatase  $\text{TiO}_2$  completely after being calcined at  $400^\circ\text{C}$  for 4 h. There still existed some characteristic peaks of metallic Ti at  $40.2^\circ$ ,  $63.1^\circ$ , and  $70.7^\circ$ , indicating that only the surface of the Ti foil reacted with NaOH, and the interior still remained as Ti metal. When Pt nanoparticles were loaded on the surface of  $\text{TiO}_2$  nanosheet porous films, the anatase phase did not change. And no apparent Pt diffraction signals appeared; this may be due to the ultrafine dispersion of Pt nanoparticles on  $\text{TiO}_2$  nanosheet porous films and its low loading amount. However, the EDS results verified that Pt nanoparticles were successfully modified on the  $\text{TiO}_2$  nanosheet porous films (as shown in Figure 1(b)); the mole ratio of Pt to  $\text{TiO}_2$  was estimated to be ca. 0.14%.

Figure 2 shows the surface morphology of the Pt-loaded  $\text{TiO}_2$  nanosheet porous films. As can be seen from Figure 2(a), anatase  $\text{TiO}_2$  film consisted of many thin nanosheets, and the surface of the film looks like porous structure. Figure 2(b) showed that some Pt nanoparticles were successfully deposited on the surface of  $\text{TiO}_2$  nanosheet porous film and were homogeneous both in size and in shape. To further observe the morphology of  $\text{TiO}_2$  film, some powders were peeled off from the substrate, and their TEM images are shown in Figures 2(c) and 2(d); we can clearly see that Pt nanoparticles are very uniform, and their particle sizes are only 3–4 nm. On one hand, the porous nanosheet structure of this kind of  $\text{TiO}_2$  film occupied larger BET surface area than the common  $\text{TiO}_2$  film obtained by the sol-gel method, so it can increase the adsorption amount of the reactive species and then accelerate the photocatalytic reaction rate. On the other hand, more irradiated light can be utilized for the porous  $\text{TiO}_2$  film because of the multiple scattering and reflection of the incident light in the channels of the porous film [17, 20, 21], so the utilization efficiency

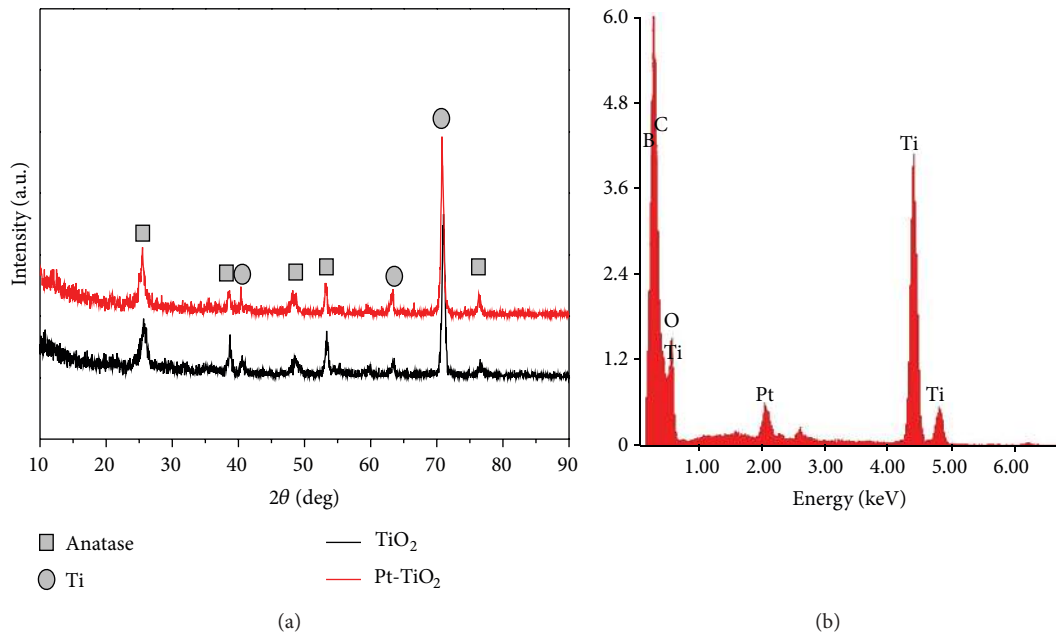


FIGURE 1: XRD patterns of TiO<sub>2</sub> and Pt-TiO<sub>2</sub> nanosheet films.

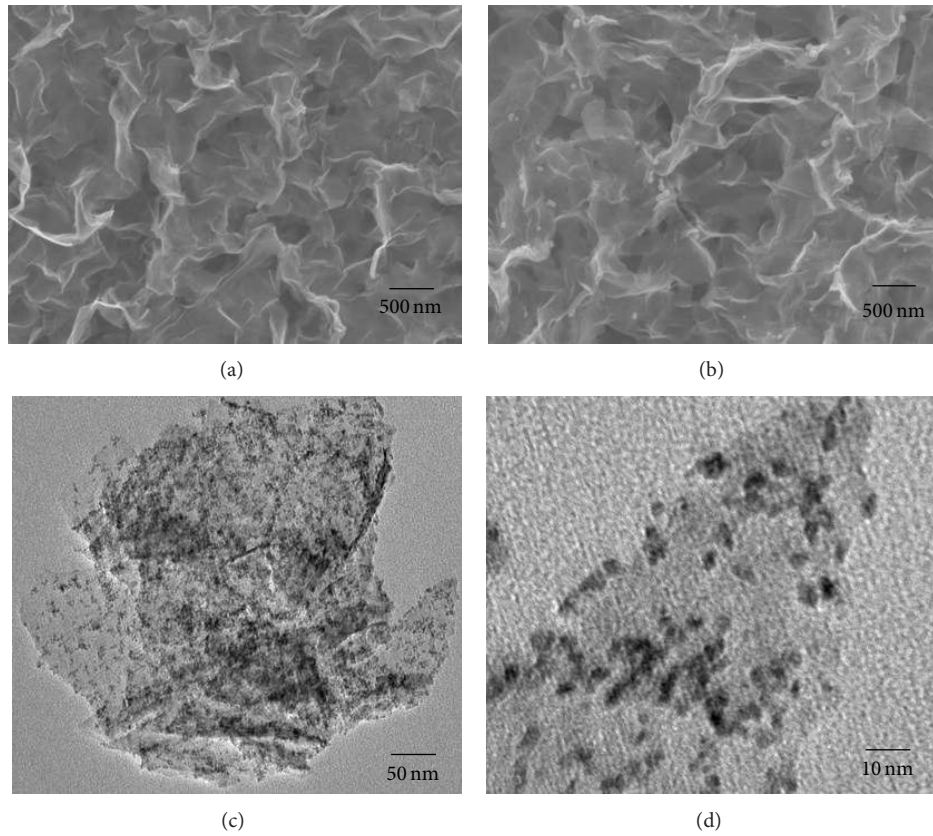


FIGURE 2: SEM images of TiO<sub>2</sub> and Pt-TiO<sub>2</sub> nanosheet films.

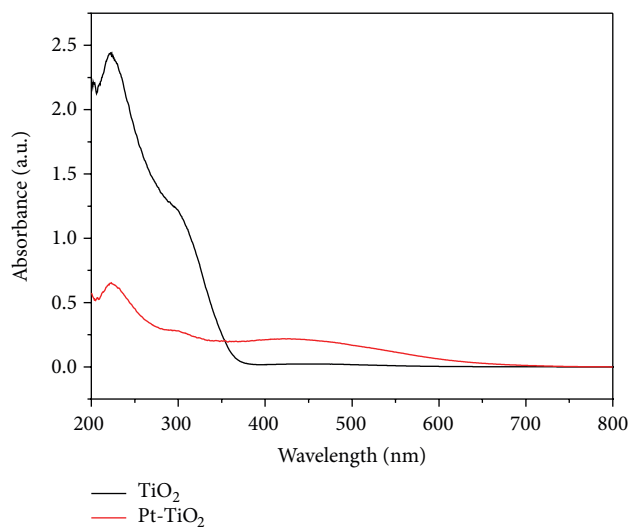


FIGURE 3: UV-vis DRS spectra of  $\text{TiO}_2$  and Pt- $\text{TiO}_2$  nanosheet films.

of the incident light was increased and thereby did favor for improving the photocatalytic activity.

The optical absorption of the nanosheet porous films was shown in Figure 3. The absorption band edge of  $\text{TiO}_2$  porous film was 380 nm. In our previous work [13, 22], we found that the onset absorption of the titanate acid was about 350–360 nm. So from the change of the absorption band, we can conclude that the titanate acid had transformed to anatase  $\text{TiO}_2$  successfully by the calcination of 400°C. While Pt nanoparticles were loaded on the surface of the  $\text{TiO}_2$  porous film, a broad peak at around 350–550 nm was observed, which should be due to the plasma resonance absorption of the Pt nanoparticles [23]. Moreover, the absorbance intensity of the film in the UV light region reduced, which should be because the loaded Pt nanoparticles shield some absorption of  $\text{TiO}_2$  nanosheets.

**3.2. Photoreduction of  $\text{CO}_2$  on Pt-Loaded  $\text{TiO}_2$  Nanosheet Porous Film.** The photoreduction of  $\text{CO}_2$  to methane was tested as a probe reaction to evaluate the photocatalytic activity of the catalyst films. As shown in Figure 4(a), the production rate of  $\text{CH}_4$  on Pt-loaded  $\text{TiO}_2$  nanosheet porous film reached 20.51 ppm/h·cm<sup>2</sup>. To confirm the photocatalytic reduction process of  $\text{CO}_2$  to  $\text{CH}_4$ , the related reference experiments were carried out. When the system was kept in dark, there was no  $\text{CH}_4$  produced, indicating that the photoexcited process of Pt-loaded  $\text{TiO}_2$  was essential in the photoreduction of  $\text{CO}_2$ . When the experiment was carried out in the absence of  $\text{H}_2\text{O}$ , almost no  $\text{CH}_4$  was detected. That implying that water is also one of the key roles for  $\text{CO}_2$  photoreduction. When a blank Ti foil with the same area of Pt-loaded  $\text{TiO}_2$  film was put into the system, the production rate of  $\text{CH}_4$  was only 1.01 ppm/h·cm<sup>2</sup>. This slow production rate of  $\text{CH}_4$  should be due to the thin oxide layer on Ti foil surface.

In addition, some comparative experiments about Pt-loaded  $\text{TiO}_2$ ,  $\text{TiO}_2$  porous film, and ordinary R- $\text{TiO}_2$  obtained by the sol-gel method proceeded. As can be seen, under the same experiment conditions, the production rate of  $\text{CH}_4$  on Pt-loaded  $\text{TiO}_2$ ,  $\text{TiO}_2$ , and R- $\text{TiO}_2$  was 20.51, 3.71, and 1.45 ppm/h·cm<sup>2</sup>, respectively. Obviously, the photocatalytic activity of the Pt- $\text{TiO}_2$  nanosheet porous film was much higher than that of  $\text{TiO}_2$  and R- $\text{TiO}_2$  film; the possible reasons were listed as follows. Firstly, it is commonly known that Pt could promote the interparticle charge migration and facilitate the photogenerated electrons transfer from conduction band of the  $\text{TiO}_2$  to Pt particles, so as to provide adequate electrons for the reduction of carbon dioxide to methane [24]. The charge carrier separation ability of Pt nanoparticles was verified by the transient photocurrent-time curve. As shown in Figure 4(b), the photocurrent density of  $\text{TiO}_2$  and Pt- $\text{TiO}_2$  nanosheet film was 0.006 and 0.017 mA·cm<sup>-2</sup>, respectively. The photocurrent density of Pt- $\text{TiO}_2$  was apparently larger than that of  $\text{TiO}_2$ , indicating that its separation efficiency of the photogenerated charge carriers was higher. Secondly, the large BET surface area and strong adsorption ability of the  $\text{TiO}_2$  nanosheet porous structure can provide more adsorption sites for  $\text{CO}_2$  molecules, so the localized concentration of  $\text{CO}_2$  on the surface of  $\text{TiO}_2$  porous film would be higher, which would accelerate the photoreduction reaction of  $\text{CO}_2$  to methane. Thirdly, the porous and incompact structure of the  $\text{TiO}_2$  nanosheet porous film would facilitate the use of more irradiated light, because more light can be scattered and reflected in the channels and pores of  $\text{TiO}_2$  film [25].

**3.3. Proposal of the Photoreduction Mechanism of  $\text{CO}_2$  to Methane on Pt-Loaded  $\text{TiO}_2$  Nanosheet Porous Film.** The photoreduction mechanism of  $\text{CO}_2$  to methane on Pt-loaded  $\text{TiO}_2$  nanosheet porous film was proposed in Figure 5. Most researchers agree that this process is based on proton-assisted multielectron transfer instead of single electron transfer, as the electrochemical potential of -2.14 V versus SCE for a single electron process is highly unfavorable [26]. When Pt-loaded  $\text{TiO}_2$  nanosheet porous film was illuminated by UV light, photon-generated electrons ( $e^-$ ) and holes ( $h^+$ ) are created on the surface of the  $\text{TiO}_2$  nanosheets. The excited holes reacted with adsorbed water molecules on the catalyst surface to produce hydroxyl radicals ( $\cdot\text{OH}$ ) and hydrogen ions ( $\text{H}^+$ ) and further oxidized by  $\cdot\text{OH}$  radicals to produce  $\text{O}_2$  and  $\text{H}^+$  [27]. And  $\text{H}^+$  would interact with the excited electrons to form  $\cdot\text{H}$  radicals. At the same time, the photo-generated electrons on the conduction band of  $\text{TiO}_2$  can be easily trapped by Pt nanoparticles because of the lower Fermi energy level of the noble metal [28], and then they would transfer rapidly to the absorbed  $\text{CO}_2$  for photoreduction reaction.  $\text{CO}_2$  molecules would interact with the excited electrons to form to  $\cdot\text{CO}_2^-$  radicals, and then reacted with  $\cdot\text{H}$  on the catalyst surface to produce  $\text{CH}_4$  [1, 28, 29]. It is known that the formation of  $\text{CH}_4$  requires eight electrons, and the enriched electron density on Pt nanoparticles would favor the formation of  $\text{CH}_4$ , which is thermodynamically

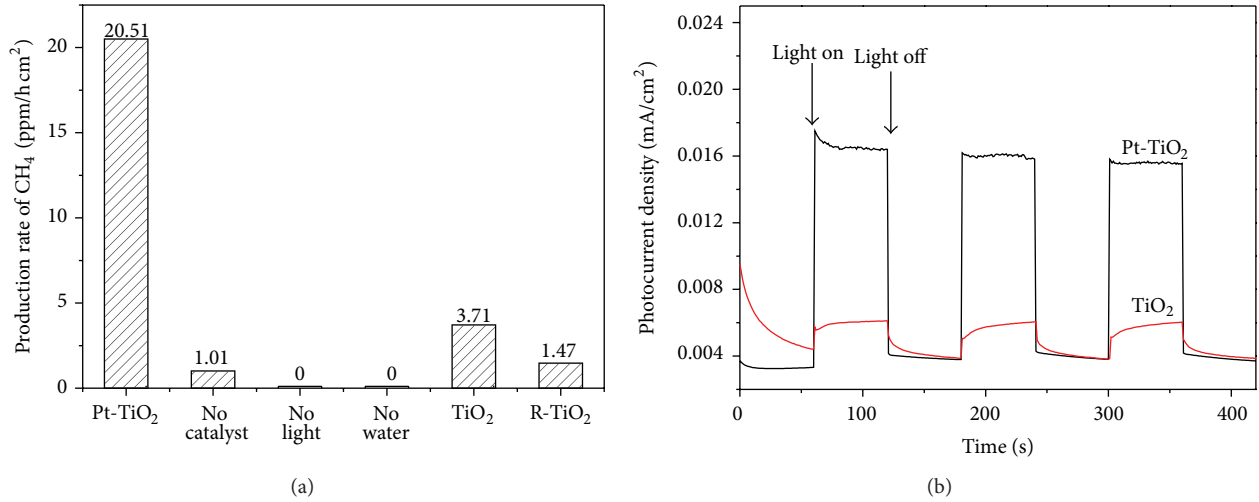


FIGURE 4: Evolution yield of  $\text{CH}_4$  and photocurrent-time curve of  $\text{TiO}_2$  and  $\text{Pt-TiO}_2$  network film under UV irradiation in same conditions.

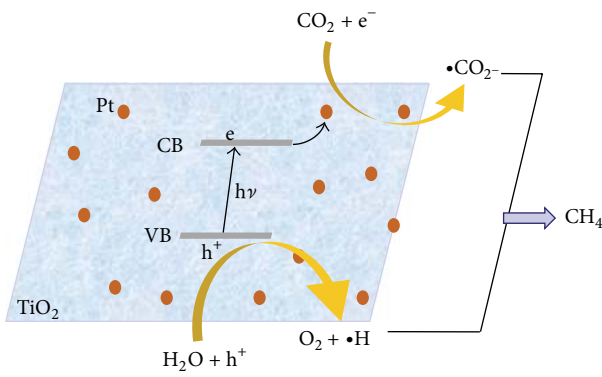
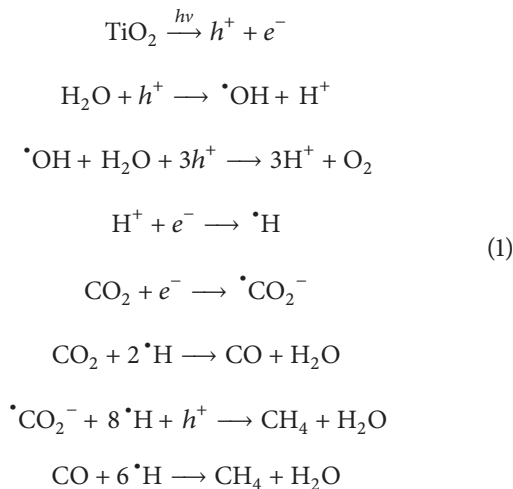


FIGURE 5: Photoreduction mechanism of  $\text{CO}_2$  to methane on Pt-loaded  $\text{TiO}_2$  nanosheet porous film.

more feasible. The possible process would have undergone the following pathway:



## 4. Conclusions

Anatase  $\text{TiO}_2$  nanosheet porous films obtained by calcination of the orthorhombic titanate acid films exhibited better performance for the photoreduction of  $\text{CO}_2$  to methane. In order to further improve the photoactivity, Pt nanoparticles with the particle size of 3-4 nm were loaded on the  $\text{TiO}_2$  porous films uniformly. The EDS results confirmed the mole ratio of Pt to  $\text{TiO}_2$  was ca. 0.14%. The conversion yield of  $\text{CO}_2$  to methane on  $\text{Pt/TiO}_2$  film reached 20.51 ppm/h·cm<sup>2</sup>. The transient photocurrent-time curves showed that the  $\text{Pt/TiO}_2$  nanosheet porous film exhibited higher photocurrent, so the higher separation efficiency of the photogenerated charge carriers should be the main reason for the high photoreduction activity of  $\text{CO}_2$ .

## Conflict of Interests

The authors declare that there is no conflict of interests regarding the publication of this paper.

## Authors' Contribution

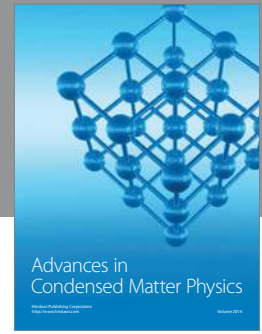
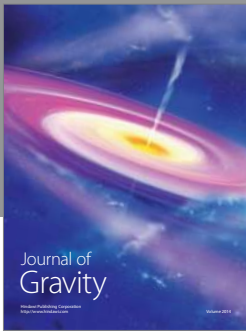
Li Qiu-ye and Zong Lan-lan contributed equally to this work.

## Acknowledgments

The authors gratefully acknowledge the support of the National Natural Science Foundation of China (no. 21103042), the Specialized Research Fund for the Doctoral Program of Higher Education (no. 20114103120001), and the Scientific Research Foundation of Henan University (no. 2010YBZR013).

## References

- [1] K. Kočí, L. Obalová, and Z. Lacný, "Photocatalytic reduction of CO<sub>2</sub> over TiO<sub>2</sub> based catalysts," *Chemical Papers*, vol. 62, pp. 1–9, 2008.
- [2] H. Yamashita, Y. Fujii, Y. Ichihashi et al., "Selective formation of CH<sub>3</sub>OH in the photocatalytic reduction of CO<sub>2</sub> with H<sub>2</sub>O on titanium oxides highly dispersed within zeolites and mesoporous molecular sieves," *Catalysis Today*, vol. 45, no. 1–4, pp. 221–227, 1998.
- [3] S. G. Zhang, Y. Fujii, H. Yamashita, K. Koyano, T. Tatsumi, and M. Anpo, "Photocatalytic reduction of CO<sub>2</sub> with H<sub>2</sub>O on Ti-MCM-41 and Ti-MCM-48 mesoporous zeolites at 328 K," *Chemistry Letters*, no. 7, pp. 659–660, 1997.
- [4] J. Rasko and F. Solymosi, "Infrared spectroscopic study of the photoinduced activation of CO<sub>2</sub> on TiO<sub>2</sub> and Rh/TiO<sub>2</sub> catalysts," *The Journal of Physical Chemistry*, vol. 98, pp. 7147–7152, 1994.
- [5] W. Lin, H. Han, and H. Frei, "CO<sub>2</sub> splitting by H<sub>2</sub>O to CO and O<sub>2</sub> under UV light in TiMCM-41 silicate sieve," *Journal of Physical Chemistry B*, vol. 108, no. 47, pp. 18269–18273, 2004.
- [6] M. Anpo, H. Yamashita, K. Ikeue et al., "Photocatalytic reduction of CO<sub>2</sub> with H<sub>2</sub>O on Ti-MCM-41 and Ti-MCM-48 mesoporous zeolite catalysts," *Catalysis Today*, vol. 44, no. 1–4, pp. 327–332, 1998.
- [7] M. Anpo, H. Yamashita, Y. Ichihashi, Y. Fujii, and M. Honda, "Photocatalytic reduction of CO<sub>2</sub> with H<sub>2</sub>O on titanium oxides anchored within micropores of zeolites: effects of the structure of the active sites and the addition of Pt," *Journal of Physical Chemistry B*, vol. 101, no. 14, pp. 2632–2636, 1997.
- [8] M. Anpo, H. Yamashita, Y. Ichihashi, and S. Ehara, "Photocatalytic reduction of CO<sub>2</sub> with H<sub>2</sub>O on various titanium oxide catalysts," *Journal of Electroanalytical Chemistry*, vol. 396, no. 1–2, pp. 21–26, 1995.
- [9] Y. J. Xu, F. M. Chen, L. Jiang, and L. D. Zhou, "Photoreduction of CO<sub>2</sub> in the suspension system of semiconductor catalyst TiO<sub>2</sub> modified by palladium," *Photochemical & Photobiological Sciences*, vol. 17, p. 61, 1999.
- [10] A. Kudo and Y. Miseki, "Heterogeneous photocatalyst materials for water splitting," *Chemical Society Reviews*, vol. 38, no. 1, pp. 253–278, 2009.
- [11] H. J. Yun, H. Lee, J. B. Joo, N. D. Kim, M. Y. Kang, and J. Yi, "Facile preparation of high performance visible light sensitive photo-catalysts," *Applied Catalysis B: Environmental*, vol. 94, pp. 241–247, 2010.
- [12] Q. Zhang, J.-B. Joo, Z. Lu et al., "Self-assembly and photocatalysis of mesoporous TiO<sub>2</sub> nanocrystal clusters," *Nano Research*, vol. 4, no. 1, pp. 103–114, 2011.
- [13] Q. Y. Li, T. Kako, and J. H. Ye, "Strong adsorption and effective photocatalytic activities of one-dimensional nano-structured silver titanates," *Applied Catalysis A: General*, vol. 375, pp. 85–91, 2010.
- [14] Q. Y. Li, T. Kako, and J. H. Ye, "PbS/CdS nanocrystal-sensitized titanate network films: enhanced photocatalytic activities and super-amphiphilicity," *Journal of Materials Chemistry*, vol. 20, pp. 10187–10192, 2010.
- [15] S. Berger, H. Tsuchiya, A. Ghicov, and P. Schmuki, "High photocurrent conversion efficiency in self-organized porous WO<sub>3</sub>," *Applied Physics Letters*, vol. 88, no. 20, Article ID 203119, 2006.
- [16] T. Kimura, N. Miyamoto, X. Meng, T. Ohji, and K. Kato, "Rapid fabrication of mesoporous titania films with controlled macroporosity to improve photocatalytic property," *Chemistry*, vol. 4, no. 9, pp. 1486–1493, 2009.
- [17] Q. Y. Li, T. Kako, and J. H. Ye, "WO<sub>3</sub> modified titanate network film: highly efficient photo-mineralization of 2-propanol under visible light irradiation," *Chemical Communications*, vol. 46, pp. 5352–5354, 2010.
- [18] X. D. Wang, X. Xue, Q. Y. Li, M. Zhang, and J. J. Yang, "Twice heat-treating to synthesize TiO<sub>2</sub>/carbon composites with visible-light photocatalytic activity," *Materials Letters*, vol. 88, pp. 79–81, 2012.
- [19] J. Yang, Z. Jin, X. Wang et al., "Study on composition, structure and formation process of nanotube Na<sub>2</sub>Ti<sub>2</sub>O<sub>4</sub>(OH)<sub>2</sub>," *Journal of the Chemical Society. Dalton Transactions*, no. 20, pp. 3898–3901, 2003.
- [20] X. Chen, J. Ye, S. Ouyang, T. Kako, Z. Li, and Z. Zou, "Enhanced incident photon-to-electron conversion efficiency of tungsten trioxide photoanodes based on 3d-photon crystal design," *ACS Nano*, vol. 5, no. 6, pp. 4310–4318, 2011.
- [21] H. Xu, X. Q. Chen, S. X. Ouyang, T. Kako, and J. H. Ye, "Size-dependent Mie's scattering effect on TiO<sub>2</sub> spheres for the superior photoactivity of H<sub>2</sub> evolution," *Journal of Physical Chemistry C*, vol. 116, pp. 3833–3839, 2012.
- [22] Q. Y. Li, X. D. Wang, Z. S. Jin et al., "n/p-Type changeable semiconductor TiO<sub>2</sub> prepared from NTA," *Journal of Nanoparticle Research*, vol. 9, pp. 951–957, 2007.
- [23] A. Gallo, M. Marelli, R. Psaro et al., "Bimetallic Au-Pt/TiO<sub>2</sub> photocatalysts active under UV-A and simulated sunlight for H<sub>2</sub> production from ethanol," *Green Chemistry*, vol. 14, no. 2, pp. 330–333, 2012.
- [24] S. J. Xie, Y. Wang, Q. H. Zhang, W. Q. Fan, W. P. Deng, and Y. Wang, "Photocatalytic reduction of CO<sub>2</sub> with H<sub>2</sub>O: significant enhancement of the activity of Pt-TiO<sub>2</sub> in CH<sub>4</sub> formation by addition of MgO," *Chemical Communications*, vol. 49, pp. 2451–2453, 2013.
- [25] Q. Y. Li, Y. Y. Xing, R. Li, L. L. Zong, X. D. Wang, and J. J. Yang, "AgBr modified TiO<sub>2</sub> nanotube films: highly efficient photo-degradation of methyl orange under visible light irradiation," *RSC Advances*, vol. 2, pp. 9781–9785, 2012.
- [26] A. J. Morris, G. J. Meyer, and E. Fujita, "Development of molecular electrocatalysts for CO<sub>2</sub> reduction and H<sub>2</sub> production/oxidation," *Accounts of Chemical Research*, vol. 42, pp. 1983–1982, 2009.
- [27] S. S. Tan, L. Zou, and E. Hu, "Photocatalytic reduction of carbon dioxide into gaseous hydrocarbon using TiO<sub>2</sub> pellets," *Catalysis Today*, vol. 115, pp. 269–273, 2006.
- [28] W. N. Wang, W. J. An, B. Ramalingam et al., "Size and structure matter: enhanced CO<sub>2</sub> photoreduction efficiency by size-resolved ultrafine Pt nanoparticles on TiO<sub>2</sub> single crystals," *Journal of the American Chemical Society*, vol. 134, pp. 11276–11281, 2012.
- [29] Q. H. Zhang, W. D. Han, Y. J. Hong, and J. G. Yu, "Photocatalytic reduction of CO<sub>2</sub> with H<sub>2</sub>O on Pt-loaded TiO<sub>2</sub> catalyst," *Catalysis Today*, vol. 148, pp. 335–340, 2009.



Hindawi

Submit your manuscripts at  
<http://www.hindawi.com>

